

Synthesis of Flame-Retardant Polypropylene/LDH-Borate Nanocomposites

Qiang Wang,^{*,†,‡} James P. Undrell,[‡] Yanshan Gao,[†] Guipeng Cai,[§] Jean-Charles Buffet,[‡] Charles A. Wilkie,[§] and Dermot O'Hare^{*,‡}

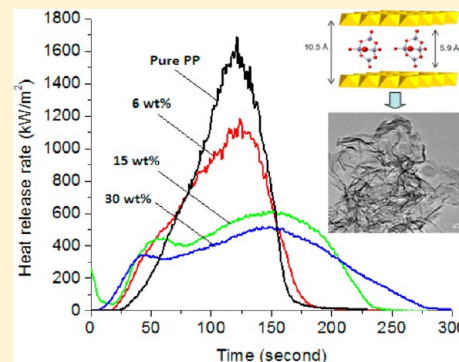
[†]College of Environmental Science and Engineering, Beijing Forestry University, 35 Qinghua East Road, Haidian District, Beijing 100083, China

[‡]Chemistry Research Laboratory, Department of Chemistry, University of Oxford, Mansfield Road, Oxford OX1 3TA, United Kingdom

[§]Department of Chemistry, Marquette University, P.O. Box 1881, Milwaukee, Wisconsin 53201, United States

S Supporting Information

ABSTRACT: New nanocomposites have been prepared using unmodified polypropylene (PP) and a new type of highly dispersed $[\text{Zn}_2\text{Al}(\text{OH})_6]\text{B}_4\text{O}_5(\text{OH})_{4.0.5}$ (Zn_2Al -borate) and $[\text{Mg}_3\text{Al}(\text{OH})_8]\text{B}_4\text{O}_5(\text{OH})_{4.0.5}$ (Mg_3Al -borate) layered double hydroxides (LDHs). PP/LDHs nanocomposites with LDH loadings of 1, 3, 6, 9, 15, and 30 wt % have been prepared by a novel solvent mixing method. Scanning electron microscopy (SEM) analysis shows that the precipitated nanocomposites materials form spherical particles with an average size of ca. 10 μm and that the LDH nanoparticles were well dispersed within the PP matrix. XRD analysis of the nanocomposites indicates that the LDHs are completely exfoliated. The thermal stability and flame retardancy properties of these new materials have been evaluated as a function of the nature of LDH and the LDH loadings. Cone calorimetry analysis indicates that PP/ Zn_2Al -borate nanocomposites exhibited superior performance than the equivalent PP/ Mg_3Al -borate nanocomposites; a 15 wt % of the highly dispersed Zn_2Al -borate LDH in PP was found to be the optimal loading. The 15% Zn_2Al -borate LDH in pristine (unmodified) PP resulted in reduction of the PHRR (peak heat release rate) (Rdctn) by 63.7%. We also demonstrated that the solvent mixing is superior to a melt mixing method. With a 6 wt % LDH loading, the reduction in PHRR is 23.8% for the melt mixing sample, which is lower than that of solvent mixing sample (29.9%), this behaviour can be attributed to the severe aggregation and poor dispersion of LDH particles.



1. INTRODUCTION

Polymer nanocomposites containing inorganic additives with layered structures have been an area of both significant academic interest and commercial importance due to their enhanced features compared to conventional composite materials.^{1–5} The additional of highly dispersed layered inorganic matrices in organic polymers have been shown to dramatically enhance the gas permeability, flame retardancy, and thermal stability of the base polymer.^{6–10} Polypropylene (PP) is the most widely used polymer for nanocomposite preparation due to its ready availability, excellent processability, and relatively low cost.^{11–15} However, PP is highly combustible, and so an improvement to the flame retardation is urgently required in order to expand its potential applications. In order to improve the flame-retardant properties of polymers, many organic and inorganic flame retardants have been developed, including halogenated organic compounds, magnesium hydroxide, aluminum hydroxide, and metal borates.^{11,16–18} Many of these flame retardants have some major shortcomings; for instance, the pyrolysis products from halogenated organic additives are considered corrosive and toxic.¹⁹ One of the

fastest growing classes of halogen-free flame retardants is the inorganic mineral-derived flame retardants: aluminum hydroxide $\{\text{Al}(\text{OH})_3, \text{ATH}\}$ and magnesium hydroxide $\{\text{Mg}(\text{OH})_2, \text{MDH}\}$. These two metal hydroxides are now widely used as flame retardants in wire coatings on cables and in building and construction applications. Although, these flame retardants offer a cost-effective solution for many low smoke zero halogen (LSZH) applications, they have some drawbacks. The most important one being the high loadings of either ATH or MDH needed to achieve the flame-retardant rating of the product. ATH and MDH are typically added in amounts of 50–70 wt % to the polymer. As a consequence, the mechanical properties of the polymer compound deteriorate and the processing becomes difficult. For some specific applications the incorporation of even higher levels of mineral flame retardants is desirable to reach certain flame-retardant specifications, but it is often simply impossible to mix these two components. This reduces

Received: May 31, 2013

Revised: June 20, 2013

Published: July 15, 2013

the wide applicability of the additives for certain LSZH applications.

Layered double hydroxides (LDHs) are emerging as a new generation of flame-retardant material. LDHs have been shown to offer good flame retardancy and smoke suppression properties due to their unique chemical composition and layered structure.^{11,20,21} During combustion, LDHs lose the interlayer water, intercalated anions, and dehydroxylate to a mixed metal oxide. These processes adsorb huge amounts of heat, dilute the concentration of O₂, promote the formation of an expanded carbonaceous coating or char on the polymer, protecting the bulk polymer from being exposed to air, and suppress smoke production due to suffocation.^{22–24} Therefore, LDH has been regarded as a promising new type of environmentally friendly flame retardant for polymer applications. Among the many different LDHs, borate intercalated LDHs have been regarded as the best candidate.²⁵ LDHs intercalated with borate anions may combine the advantages of both Mg(OH)₂, Al(OH)₃, and zinc borate. In addition to its high efficiency, borate intercalated LDHs are halogen-free and nontoxic.

Previously, the solvent-based preparation of LDH/polymer nanocomposites has required either the LDH to be intercalated with organic anions (organo-LDH) or the polymer needs to be modified with polar substituents.^{26–29} This is to facilitate the miscibility between the typically hydrophobic polymer and the hydrophilic LDHs; however, both methods have serious limitations as well as the additional cost and complexity of the process.³⁰ These limitations include unwanted change in the polymer characteristics, a limited selection of anions that can be intercalated, and the fact that organo-LDHs have low decomposition temperatures. The main benefit of employing a solvent-based synthesis method is the formation of a true nanocomposite with excellent dispersion of the LDH compared to the traditional melt mixing synthesis method. The drying of the LDH dispersion before melt mixing inevitably results in LDH particle aggregation, and so melt mixing of an LDH and the polymer results in a inferior LDH dispersion compared to a solvent-based synthesis.⁸ Until recently, it was widely believed that inorganic-LDHs containing inorganic anions such as borate, CO₃^{2–}, and Cl[–] cannot be dispersed in nonpolar solvents due to their high hydrophilicity. For this reason, LDH-borate, which is one of the most efficient flame-retardant fillers, has not been successfully introduced into polymers using the solvent mixing method.

Recently, we have reported an aqueous miscible organic solvent treatment (AMOST) method for the synthesis of stable, transparent dispersions of the hydrophilic LDHs in nonpolar solvents.^{31,32} This technique can tune the surface of LDHs to be hydrophobic, enable them to be highly dispersible in nonpolar solvents such as xylene, and make it possible to prepare PP/inorgano-LDHs nanocomposites using solvent mixing method for the first time ever.³² The technique has been extended to the synthesis of highly porous and highly dispersed Zn₂Al-borate and Mg₃Al-borate LDHs.³¹ Here we report the use of Zn₂Al-borate and Mg₃Al-borate LDH dispersions in nonpolar hydrocarbons to prepare low smoke, zero halogen containing flame-retardant PP/LDH nanocomposites.

2. EXPERIMENTAL DETAILS

2.1. Synthesis of Materials. *Synthesis of Solvent Dispersed LDHs.* Zn₂Al-borate LDH was initially crystallized by adding a 50 mL

aqueous solution containing 11.14 g of Zn(NO₃)₂·6H₂O (0.0375 mol) and 7.025 g of Al(NO₃)₃·9H₂O (0.0187 mol) dropwise into a 50 mL aqueous solution containing 5.225 g of H₃BO₃ (0.085 mol). The pH of the precipitation solution was controlled at ca. 8.3 using a NaOH (1 M) solution. During the whole synthesis, the system was protected with N₂ gas to prevent the contamination by atmospheric CO₂. The precipitated LDH slurry was filtered and washed with H₂O until pH = 7 (use around 500 mL of H₂O). Then, the neutral pH aqueous LDH slurry was redispersed in acetone and stirred at room temperature for 1 h. Finally, the prepared [Zn₂Al(OH)₆][B₄O₅(OH)₄]_{0.5} (Zn₂Al-borate LDH) was dried at 65 °C overnight. Mg₃Al-borate LDH was initially precipitated in water at pH 9 by adding 100 mL of an aqueous solution containing Mg(NO₃)₂·6H₂O (0.075 mol) and Al(NO₃)₃·9H₂O (0.025 mol) dropwise into a 100 mL aqueous solution containing H₃BO₃ (0.187 mol). The precipitated LDH slurry was filtered and washed with H₂O until pH = 7 (use around 500 mL of H₂O). Then, the neutral pH aqueous LDH slurry was redispersed in acetone and stirred at room temperature for 1 h. Finally, the prepared [Mg₃Al(OH)₈][B₄O₅(OH)₄]_{0.5} (Mg₃Al-borate) was dried at 65 °C overnight.

Synthesis of PP/LDH Nanocomposites. 5 g of PP was added to a 250 mL round-bottom flask containing 100 mL of xylene. A slurry of the LDH prepared above in acetone was then added to the flask. The amount of the LDH slurry added to the PP was adjusted to give LDH loadings of 1, 3, 6, 9, 15, and 30 wt %. The mixture was refluxed at approximately 140 °C for 2 h to enable the dissolution of the all the PP. After the reflux process was complete, the hot xylene solution containing dissolved PP and the highly dispersed LDH nanoparticles was poured into 100 mL of hexane (also called a solvent extraction method) in order to precipitate the PP/LDH nanocomposite. The PP/LDH nanocomposites were isolated by filtration and dried in a vacuum-oven.

Synthesis of PP/LDH Nanocomposites by the Melt Mixing Method. Dried Zn₂Al-borate LDHs powders and PP pellets were combined in a Brabender mixer (KEDSE 12/36) at a temperature of 120 °C with a screw speed of 60 rpm for 8 min.

2.2. Characterization Techniques. **XRD.** XRD patterns were recorded on a PANalytical X'Pert Pro instrument in reflection mode with Cu Kα radiation. The accelerating voltage was set at 40 kV with 40 mA current (λ = 1.542 Å) at 0.01° s^{–1} from 1 to 70° with a slit size of 1/4°.

SEM and SEM-EDX. SEM and SEM-EDX analyses were performed on a JEOL JSM 6100 scanning microscope with an accelerating voltage of 20 kV. Powder samples were spread on carbon tape adhered to an SEM stage. Before observation, the samples were sputter-coated with a thin platinum layer to prevent charging and to improve the image quality.

Thermal Stability. The thermal stability of neat PP and its nanocomposites was studied by TGA (Netzsch), which was carried out with a heating rate of 10 °C/min in an air flow rate of 50 mL/min from 25 to 600 °C.

Flame Retardancy. The flame-retardant performance of prepared PP/Zn₂Al-borate nanocomposites was evaluated using a cone calorimetry (Atlas Cone 2 instrument). Approximately 30 g of nanocomposite samples was compression molded into 10 cm × 10 cm square plaques of uniform thickness (~3 mm) before the tests were performed. A cone-shaped heater with incident flux of 35 kW/m² was used, and the spark was continuous until the sample ignited. All samples were run in triplicate, and the average value with standard deviation is reported. The results from cone calorimeter are generally considered to be reproducible to ±10%.

3. RESULTS AND DISCUSSION

3.1. Synthesis and Characterization of PP/LDH Nanocomposites. We have recently reported that an aqueous miscible organic solvent treatment (AMOST) method enables us to prepare highly porous and highly dispersed hydrophobic Zn₂Al-borate and Mg₃Al-borate LDHs materials.³¹ Dinitrogen BET analysis indicated that these LDHs possess specific surface areas of 458.6 and 263 m²/g with specific pore volumes of 2.15

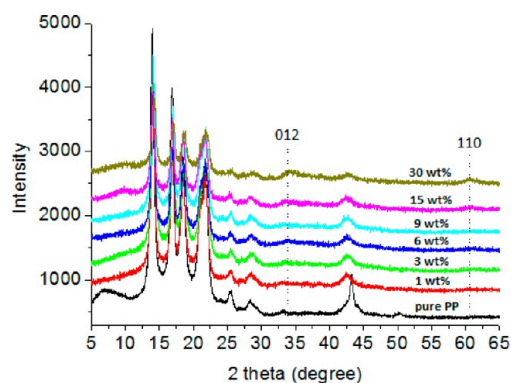


Figure 1. XRD patterns of pure PP and PP/Zn₂Al-borate nanocomposites with various LDH loadings.

and 1.07 cm³/g, respectively.³¹ SEM images in Figures S1 and S2 suggest that the acetone-treated LDHs have much smaller particle size and better dispersion. TEM analyses show that these high surface areas are due to the highly exfoliated nature of the LDHs; the samples consist of individual LDH nanosheets that show no tendency to aggregate on drying (Figure S3). These LDHs redisperse in most organic solvents giving clear, stable dispersions. These dispersions can then be readily used to make polymer/LDH composites by simply dissolving the polymer in a suitable solvent, adding the LDH dispersion, and then precipitating the composition from solution, i.e., solvent mixing method.

Using this approach, we were able to make a range of PP/Zn₂Al-borate and PP/Zn₂Al-borate nanocomposites with range of loadings from 1–30 wt %. Figure 1 shows the XRD patterns of PP/Zn₂Al-borate nanocomposites with various loadings of 1, 3, 6, 9, 15, and 30 wt %. Unlike many other reported polymer/LDH nanocomposites, the XRD reflections due to the

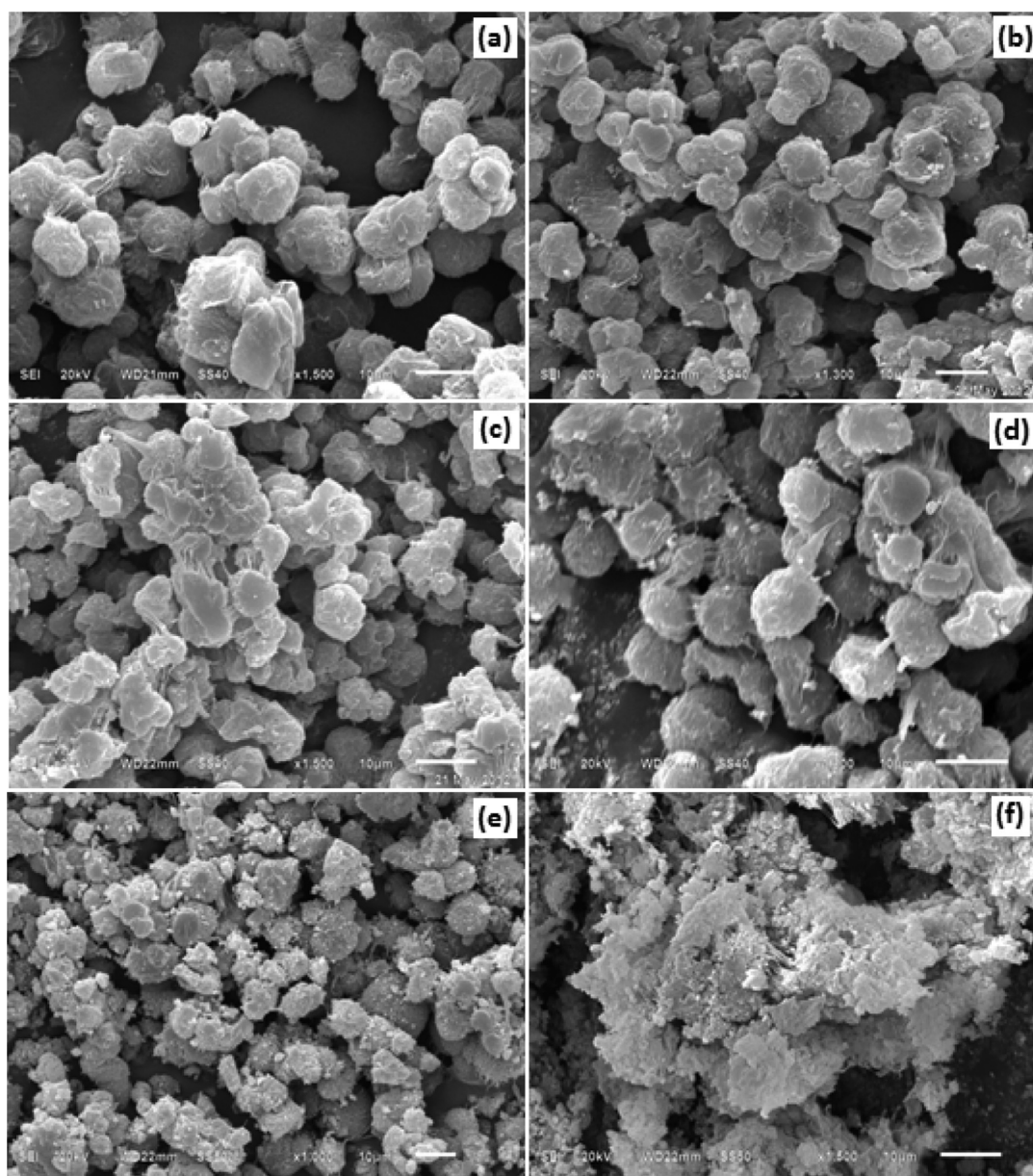


Figure 2. SEM images of PP/Zn₂Al-borate LDH nanocomposites with various loadings: (a) 1, (b) 3, (c) 6, (d) 9, (e) 15, and (f) 30 wt %.

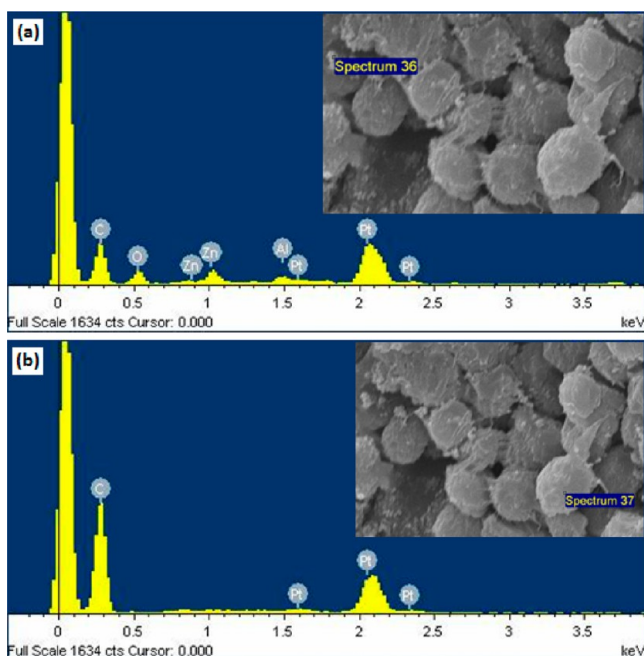


Figure 3. EDX analysis of PP/Zn₂Al-borate LDH nanocomposite.

Table 1. Cone Calorimetry Data for PP/LDH Nanocomposites Tested at 35 kW/m² ^a

nanocomposite	PHRR (kW/m ²)	RDCTN (%)	THR (MJ/m ²)	AMLR (g/(m ² s))	Char (wt %)
PP	1693.0	NA	108.5	28.2	0
6 wt % PP/Mg ₃ Al-borate	1290.3	23.8	104.2	22.7	0.3
6 wt % PP/Zn ₂ Al-borate	1186.9	29.9	98.8	21.6	0.6
15 wt % PP/Zn ₂ Al-borate	614	63.7	95.4	12.7	9.5
30 wt % PP/Zn ₂ Al-borate	517.4	69.4	84.7	10.3	17.8

^aPHRR = peak heat release rate; RDCTN = % reduction in PHRR; THR = total heat release; AMLR = average mass loss rate (10–90%); Char (wt %) = final mass/initial mass.

inorganic additive are not observed even with LDH loading as high as 30 wt %. In particular, we observe no 00 l ($l = 3, 6, 9$) Bragg reflections due to the stacking of individual LDH layers. At the 30 wt % loading we observed two very weak Bragg reflections at $2\theta = 33.0^\circ$ and 60.6° , which can be assigned to the (012) and (110) reflections of the individual LDH layers. The XRD data suggest that the Zn₂Al-borate LDHs are exfoliated and well dispersed within the PP matrix. Figure 2 shows the SEM images of PP/Zn₂Al-borate LDHs with various loadings (1, 3, 6, 9, 15, and 30 wt %). Spherical particles with an average size of ca. 10 μm were formed for all nanocomposites except the one with 30 wt %, which is caused by the rapid precipitation of the polymer composite in hexane. When the LDH loading is low (<9 wt %), aggregated LDH particles can rarely be observed, which can be attributed to the ultrafine LDH particles and its good dispersion within PP matrix. When the LDH loading is higher (>9 wt %), nanosized LDH particles were observed on the surface of PP spherical particles, and the amount increased with the increase in LDH loadings. Particularly with 30 wt % loading, there were so many LDH nanoparticles present that spherical PP particles could not be formed. This result clearly indicated that these nanosized LDH

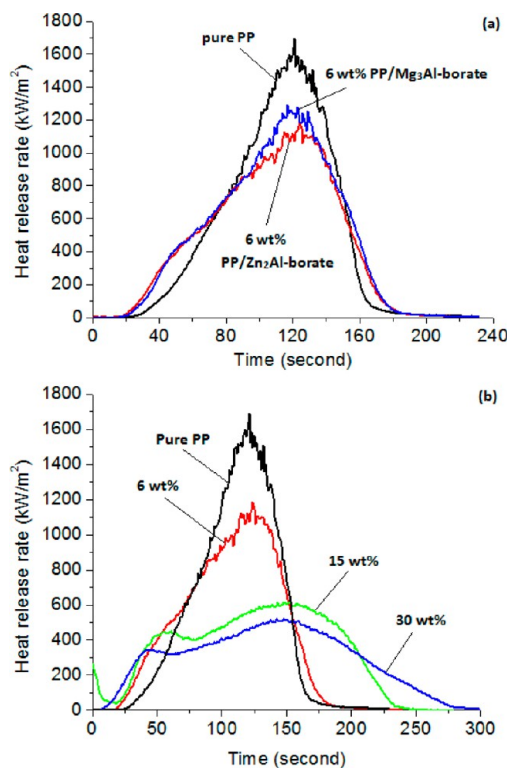


Figure 4. (a) Heat release rate (HRR) of pure PP, 6 wt % PP/Mg₃Al-borate LDH nanocomposite, and 6 wt % PP/Zn₂Al-borate LDH nanocomposite. (b) HRR of PP/Zn₂Al-borate nanocomposites with various LDH loadings (0, 6, 15, and 30 wt %).

particles were well dispersed within the PP matrix up to a loading of 15 wt %. Similar results were also observed with PP/Mg₃Al-borate nanocomposites. In order to confirm that the surface nanoparticles are Zn₂Al-borate LDH, SEM-EDX was utilized. Figure 3a shows the EDX elemental analysis of a representative surface nanoparticle, from which both Zn and Al were detected, while the EDX elemental analysis of a representative PP particle in Figure 3b clearly indicated that only C can be detected.

3.2. Flame Retardant and Thermal Stability of PP/LDH Nanocomposites. Cone calorimetry is the most important tool for assessing flammability behavior of polymer composites. This provides the peak heat release rate (PHRR), total heat released (THR), average mass loss rate (AMLR) and char yield. The cone calorimetry data are summarized in Table 1, and the plots of heat release rate versus time are shown in Figure 4. To compare the effectiveness of flame retardants in nanocomposites, the reduction in PHRR is the most important parameter obtained from cone calorimetry, which gives a general indication on the size of the fire and how fast it grows. Table 1 and Figure 4 indicate that the addition of LDHs reduces the PHRR significantly. For pure PP, its PHRR was determined as 1693 kW/m². However, after adding only 6 wt % of Mg₃Al-borate or Zn₂Al-borate LDH, the PHRR was decreased to 1290.3 and 1186.9 kW/m², respectively. As a flame-retardant additive, Zn₂Al-borate is more efficient than Mg₃Al-borate. Figure 4b indicates that a much more significant reduction in PHRR can be achieved by increasing the LDH loadings. With 15 and 30 wt % of Zn₂Al-borate LDH, the reduction in PHRR was 63.7 and 69.4%, respectively. Although high loadings are not necessarily cost-effective, it is common in

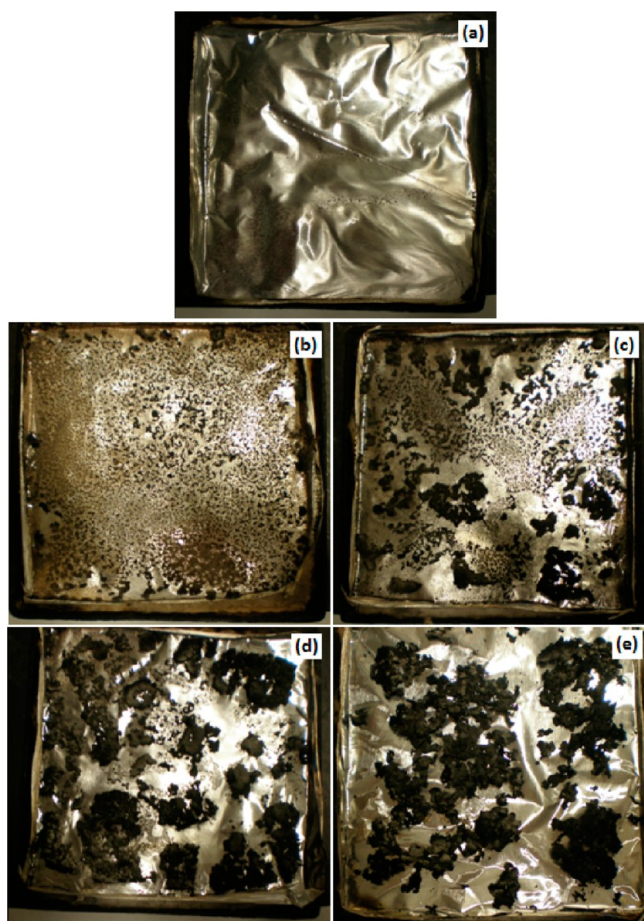


Figure 5. Residual ash formation in cone calorimetry tests of (a) pure PP, (b) 6 wt % PP/Mg₃Al-borate, (c) 6 wt % PP/Zn₂Al-borate, (d) 15 wt % PP/Zn₂Al-borate, and (e) 30 wt % PP/Zn₂Al-borate.

industry to have flame-retardant loadings of up to 60 wt %;³³ 15–30 wt % LDH loading can therefore still be considered industrially viable. Importantly, not only the PHRR but also the THR and the AMLR were significantly decreased. With 15 and 30 wt % of Zn₂Al-borate LDH, the THR was decreased from 108.5 MJ/m² for pure PP to 95.4 and 84.7 MJ/m², respectively, and the AMLR was decreased from 28.2 g/(m² s) for pure PP to 12.7 and 10.3 g/(m² s), respectively. This results demonstrated that the presence of Zn₂Al-borate LDH has promoted incomplete combustion of the nanocomposite.³⁴

After cone calorimetry tests, the formation of a residual char was observed for all samples except pure PP (Figure 5). The char can act as a barrier to both heat and mass transfer which makes it more difficult for degrading material to escape to the vapor phase and also prevents heat transfer back to the polymer.¹¹ The PP/Zn₂Al-borate LDH nanocomposite produced more char than PP/Mg₃Al-borate LDH nanocomposite. As it was expected, the quantity of char produced increased with increasing Zn₂Al-borate loading and corroborates the decreases in PHRR and THR observed at higher LDH loadings.

In addition, PP/Zn₂Al-borate LDH nanocomposite was also prepared using the melt mixing method. Figure 6a shows the comparison of the heat release rate of PP/Zn₂Al-borate nanocomposite synthesized by solvent mixing and melt mixing methods. It is obvious that the solvent mixing is superior to melt mixing method. With 6 wt % of LDH, the reduction in PHRR is 23.8% for melt mixing sample and 29.9% for solvent

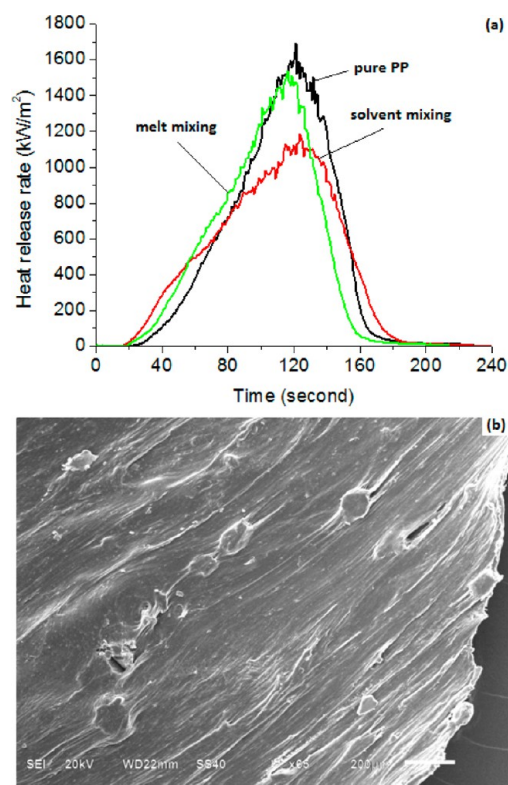


Figure 6. (a) Comparison of the HRR of 6 wt % PP/LDH nanocomposites synthesized using solvent mixing and melt mixing methods. (b) SEM image of 6 wt % PP/Zn₂Al-borate nanocomposites synthesized using the melt mixing method.

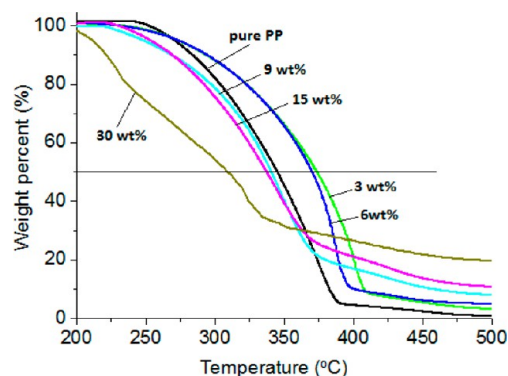


Figure 7. TGA analysis of PP/Zn₂Al-borate nanocomposites with various LDH loadings (0, 3, 6, 9, 15, and 30 wt %).

Table 2. TGA Data for the PP/LDH Nanocomposites in Air

properties	PP/Zn ₂ Al-borate						
LDH loading (wt %)	0	1	3	6	9	15	30
T _{0.1} (°C)	284	257	294	295	269	269	222
T _{0.5} (°C)	345	358	374	370	341	337	309
total weight loss (wt %)	100	99.5	97.6	95.9	93.1	89.8	81.2

mixing sample. Figure 6b shows the SEM image of PP/Zn₂Al-borate LDH nanocomposite synthesized by the melt mixing method. Big LDH particles with an average size of 60–100 μm were clearly seen, which confirms that the melt mixing method resulted in much worse dispersion of LDHs. It is well established that introducing LDH fillers may affect the thermal

stability of PP. The influence of various LDH loadings on the thermal stability of PP was investigated by TGA, as shown in Figure 7 and Table 2. When the LDH loading is no higher than 3 wt %, the 50% weight loss temperature ($T_{0.5}$) increased with the increase in LDH loadings. The $T_{0.5}$ was increased by 29 °C with 3 wt % Zn_2Al -borate LDH. While when the LDH loading is higher than 3 wt %, $T_{0.5}$ starts to decrease gradually with the increase in LDH loadings. Luckily, the $T_{0.5}$ was only slightly decreased with 15 wt % LDH addition. Therefore, it is easy to conclude that 15 wt % is the optimal LDH loading, with which both the flame-retardant performance and the thermal stability of the nanocomposites are good. If the LDH loading is too high (e.g., 30 wt %), the thermal stability of the nanocomposites became lower and it is not favorable for practical applications.

4. CONCLUSIONS

A novel method of preparing highly dispersed suspensions of the LDHs in nonpolar solvents enables the synthesis of PP/LDH-borate nanocomposites using unmodified PP. PP/ Zn_2Al -borate and PP/ Mg_3Al -borate nanocomposites with various LDH loadings have been prepared. XRD analysis of these nanocomposites confirmed that the LDH was exfoliated during the synthesis and is well dispersed in the PP. TGA analysis of the PP/LDH nanocomposites showed they had increased thermal stability. Cone calorimetry analysis was performed on all the PP/LDH nanocomposites; we found that the flame-retardancy properties of the materials prepared using the solvent mixing to be superior to those prepared using a melt mixing method. With 15 wt % of highly dispersed Zn_2Al -borate LDH in PP, a PHRR reduction of 63.7% compared to PP was achieved. We anticipate the AMOST method used in this contribution might be applicable to other kinds of clays and make a significant impact across a wide range of applications. Considering that very low LDH loading (15 wt %) can result in excellent flame-retardant properties, many new applications of these nanocomposites can be expected.

■ ASSOCIATED CONTENT

Supporting Information

Figures S1–S3. This material is available free of charge via the Internet at <http://pubs.acs.org>.

■ AUTHOR INFORMATION

Corresponding Author

*E-mail qiang.wang.ox@gmail.com, qiangwang@bjfu.edu.cn, Tel +8613699130626 (Q.W.); e-mail dermot.ohare@chem.ox.ac.uk, Tel +44-1865 272686 (D.O.).

Notes

The authors declare no competing financial interest.

■ ACKNOWLEDGMENTS

This work is supported by the Fundamental Research Funds for the Central Universities (TD-JC-2013-3), the Program for New Century Excellent Talents in University (NCET-12-0787), the Key Laboratory of Functional Inorganic Material Chemistry (Heilongjiang University), Ministry of Education, and SCG Chemicals Ltd, Bangkok, Thailand.

■ REFERENCES

- (1) Alsewilem, F. D. *Open Macromol. J.* **2012**, *6*, 19.
- (2) O'Leary, S.; O'Hare, D.; Seeley, G. *Chem. Commun.* **2002**, 1506.
- (3) Zhu, J.; Zhang, X.; Haldolaarachchige, N.; Wang, Q.; Luo, Z.; Ryu, J.; Young, D. P.; Wei, S.; Guo, Z. *J. Mater. Chem.* **2012**, *22*, 4996.
- (4) Wei, S.; Mavinakuli, P.; Wang, Q.; Chen, D.; Asapu, R.; Mao, Y.; Haldolaarachchige, N.; Young, D. P.; Guo, Z. *J. Electrochem. Soc.* **2011**, *158*, K205.
- (5) Li, Y.; Zhu, J.; Wei, S.; Ryu, J.; Wang, Q.; Sun, L.; Guo, Z. *Macromol. Chem. Phys.* **2011**, *212*, 2429.
- (6) Taviot-Gueho, C.; Leroux, F. *Struct. Bonding (Berlin)* **2006**, *119*, 121.
- (7) Wang, L.; He, X.; Wilkie, C. A. *Materials* **2010**, *3*, 4580.
- (8) Wang, Q.; Zhang, X.; Wang, C. J.; Zhu, J.; Guo, Z.; O'Hare, D. J. *Mater. Chem.* **2012**, *22*, 19113.
- (9) Leroux, F.; Gueho, C. T. J. *Mater. Chem.* **2005**, *15*, 3628.
- (10) Nshuti, M. C.; Wang, D. Y.; Hossenlopp, J. M.; Wilkie, C. A. J. *Mater. Chem.* **2008**, *18*, 3091.
- (11) Wang, L.; He, X.; Lu, H.; Feng, J.; Xie, X.; Su, S.; Wilkie, C. A. *Polym. Adv. Technol.* **2011**, *22*, 1131.
- (12) Edwards, K. L. *Mater. Des.* **2004**, *25*, 529.
- (13) Sun, L.; Liu, J.; Kirumakki, S. R.; Schwerdtfeger, E. D.; Howell, R. J.; Al-Bahily, K.; Miller, S. A.; Clearfield, A.; Sue, H.-J. *Chem. Mater.* **2009**, *21*, 1154.
- (14) Zhu, J.; He, Q.; Luo, Z.; Khasanov, A.; Li, Y.; Sun, L.; Wang, Q.; Wei, S.; Guo, Z. *J. Mater. Chem.* **2012**, *22*, 15928.
- (15) Kaspersma, J.; Doumen, C.; Munro, S.; Prins, A. M. *Polym. Degrad. Stab.* **2002**, *77*, 325.
- (16) Zhang, G.; Ding, P.; Zhang, M.; Qu, B. *Polym. Degrad. Stab.* **2007**, *92*, 1715.
- (17) Lv, J.; Qiu, L.; Qu, B. *Nanotechnology* **2004**, *5* (11), 1576.
- (18) Marosfoi, B. B.; Garas, S.; Bodzayl, B. *Polym. Adv. Technol.* **2008**, *19*, 693.
- (19) Key, P. B.; Chung, K. W.; Hoguet, J.; Shaddix, B.; Fulton, M. H. *Sci. Total Environ.* **2008**, *399*, 28.
- (20) Leroux, F.; Besse, J. P. *Chem. Mater.* **2011**, *13*, 3507.
- (21) Zammarrano, M.; Franceschi, M.; Bellayer, S.; Gilman, J. W.; Meriani, S. *Polymer* **2005**, *46*, 9314.
- (22) Xu, S.; Zhang, L.; Lin, Y.; Li, R.; Zhang, F. J. *Phys. Chem. Solids* **2012**, *73*, 1514.
- (23) Costantino, U.; Gallipoli, A.; Nocchetti, M.; Camino, G.; Bellucci, F.; Frache, A. *Polym. Degrad. Stab.* **2005**, *90*, 586.
- (24) Evans, D. G.; Duan, X. *Chem. Commun.* **2006**, 485.
- (25) Shi, L.; Li, D.; Wang, J.; Li, S.; Evans, D. G.; Duan, X. *Clays Clay Miner.* **2005**, *53*, 294.
- (26) Costa, F. R.; Saphiannikova, M.; Wagenknecht, U.; Heinrich, G. *Adv. Polym. Sci.* **2008**, *210*, 101.
- (27) Costa, F. R.; Abdel-Goad, M.; Wagenknecht, U.; Heinrich, G. *Polymer* **2005**, *46*, 4447.
- (28) Lonkar, S. P.; Morlat-Therias, S.; Caperaa, N.; Leroux, F.; Gardette, J. L.; Singh, R. P. *Polymer* **2009**, *50*, 1505.
- (29) Wang, Q.; O'Hare, D. *Chem. Rev.* **2012**, *112*, 4124.
- (30) Chen, W.; Qu, B. *Chem. Mater.* **2003**, *15*, 3208.
- (31) Wang, Q.; O'Hare, D. *Chem. Commun.* **2013**, *49*, 6301.
- (32) Wang, Q.; Zhang, X.; Zhu, J.; Guo, Z.; O'Hare, D. *Chem. Commun.* **2012**, *48*, 7450.
- (33) Mai, K.; Qiu, Y.; Lin, Z. J. *Appl. Polym. Sci.* **2003**, *88*, 2139.
- (34) Hu, Y.; Song, L. *Flame Retardant Polymer Nanocomposites*; John Wiley & Sons, Inc.: New York, 2007.